FACULTY OF MECHANICAL AND CIVIL ENGINEERING
IN KRALJEVO
UNIVERSITY OF KRAGUJEVAC

X Triennial
International Conference

HEAVY MACHINERY HM 2021

Proceedings

VRNJAČKA BANJA, SERBIA
June 23 - June 25 2021

Contribution to the problem of in-plane vibration of circular arches with varying cross-sections

Slaviša Šalinić[1*], Aleksandar Obradović[2]
[1]Faculty of Mechanical and Civil Engineering/Department, University of Kragujevac, Kraljevo (Serbia)
[2]Faculty of Mechanical Engineering /Mechanics, University of Belgrade, Belgrade (Serbia)

Free in-plane vibration analysis of circular arches with varying cross-sections is studied by means of the symbolic-numeric method of initial parameters. The effects of axial extension, transverse shear deformation and rotatory inertia are considered. For various boundary conditions, natural frequencies of free in-plane vibration of circular arches with varying cross-sections are obtained. By comparing obtained results with previous ones available in the literature the effectiveness of application of the symbolic-numeric method of initial parameters to the problem considered is proven.

Keywords: Circular arch, Free vibration, Varying cross-section, Natural frequencies

1. INTRODUCTION

The circular arches represent important components of engineering structures. The vibration analysis of circular arches is one of important aspect of dynamic analysis of these structural components. The review of papers on this topic can be found in [1-4]. In the literature, the three principal dynamical models of circular arches were considered: the model with included the effects of axial extensibility, shear deformation and rotary inertia [5-11] (the so-called Timoshenko circular arches); the model with neglected the effects of both shear deformation and rotary inertia [12-15]; the model without the effects of axial extensibility, shear deformation and rotary inertia [16,17] (the so-called Euler-Bernoulli circular arches). The exact solution of the vibration problem of uniform Timoshenko circular arches was given in [6] and for stepped ones in [7]. Based on these solutions the approximate approach for vibration analysis of tapered Timoshenko circular arches was presented in [9]. Note that the similar idea is used in the approach for vibration analysis of tapered Euler-Bernoulli circular arches was given in [16]. The papers [10, 19-23] are interesting in that they consider the influence of functionally graded material on the vibration characteristics of circular arches.

The aim of this paper is to evaluate a method for the vibration analysis of tapered circular Timoshenko arches. The method is based on the use of the symbolic-numeric method of initial parameters [24]. To the authors' best knowledge of the literature, the method presented was not considered so far in scientific papers.

2. FORMULATION OF GOVERNING EQUATIONS

Figure 1 shows a thin elastic circular arch with varying cross-section in its undeformed configuration. Without loss of generality, it is assumed that the arch has a rectangular cross-section of constant width b and variable height h which is a function of the angular coordinate θ.

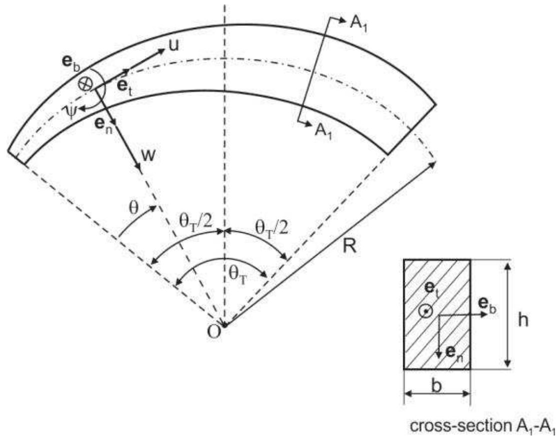

Figure 1: The geometry of a circular arch with varying cross-section

By the angle θ a point on the arch centroidal curve is defined. Also, the following quantities are shown in Figure 1: $\mathbf{e}_t$, $\mathbf{e}_n$, and $\mathbf{e}_b$ are the unite vectors of tangent, principal normal, and binormal of the arch centroidal curve, respectively; R is the radius of the undeformed centroidal curve of the arch; θ_T is the opening angle of the arch, w represents the radial displacement of a point of the centroidal curve in the $\mathbf{e}_n$ direction; u represents the tangential displacement of a point of the centroidal curve in the $\mathbf{e}_t$ direction; ψ is the angle of rotation of the arch cross-section due to bending. The circular arch is made of a homogeneous material of the modulus of elasticity E, the mass density ρ, and the shear modulus G. It is taken that $\theta = 0$ at the arch left end.

The corresponding governing differential equations of the free in-plane vibrations of the circular arch considered read [9]:

*Corresponding author: Slaviša Šalinić, Dositejeva 19, Kraljevo, salinic.s@mfkv.kg.ac.rs

$$\frac{dU}{d\theta}=W+\frac{R}{EA(\theta)}N\,, \tag{1}$$

$$\frac{dW}{d\theta}=-U+\frac{R}{GA(\theta)k}Q+R\Psi\,, \tag{2}$$

$$\frac{d\Psi}{d\theta}=\frac{R}{EI_b(\theta)}M_b\,, \tag{3}$$

$$\frac{dM_b}{d\theta}=-RQ-R\rho\omega^2 I_b(\theta)\Psi\,, \tag{4}$$

$$\frac{dN}{d\theta}=Q-R\rho A(\theta)\omega^2 U\,, \tag{5}$$

$$\frac{dQ}{d\theta}=-N-R\rho A(\theta)\omega^2 W\,. \tag{6}$$

where W and U are the mode shape functions corresponding to the radial and tangential displacements, w and u, respectively, N, Q, and M_b are the mode shape functions of axial forces, shear forces, and bending moments at an arch cross-section, respectively, k is the shear correction factor, and ω is the natural angular frequency of free in-plane vibration of the circular arch. In this paper, it is taken $k=5/6$ for the rectangular cross-sections. The other expressions for the coefficient k may be found in [25].

For the purpose of further exposition, let us introduce the following dimensionless quantities:

$$\xi=\frac{\theta}{\theta_T},\quad \overline{U}=\frac{U}{R},\quad \overline{W}=\frac{W}{R}, \tag{7}$$

$$r=\frac{I_{br}}{A_r R^2},\quad \overline{A}(\xi)=\frac{A(\theta)}{A_r},\quad \overline{I}_b(\xi)=\frac{I_b(\theta)}{I_{br}}, \tag{8}$$

$$\mu=\frac{E}{Gk}=\frac{2(1+v)}{k},\quad \overline{N}=\frac{N}{EA_r},\quad \overline{Q}=\frac{QR^2}{EI_{br}}, \tag{9}$$

$$\overline{M}_b=\frac{M_b R}{EI_{br}},\quad \frac{d}{d\theta}=\frac{1}{\theta_T}\frac{d}{d\xi}, \tag{10}$$

where v is the Poisson's ratio and A_r and I_{br} are the cross-sectional area and the cross-sectional area moment of inertia about axis $\mathbf{e}_b$, respectively, at a reference cross-section.

Using (7)-(10) the equation system (1)-(6) can be written in the following dimensionless form:

$$\frac{d\overline{U}}{d\xi}=\theta_T\overline{W}+\frac{\theta_T}{\overline{A}(\xi)}\overline{N}, \tag{11}$$

$$\frac{d\overline{W}}{d\xi}=-\overline{U}\theta_T+\frac{\theta_T r\mu}{\overline{A}(\xi)}\overline{Q}+\theta_T\Psi, \tag{12}$$

$$\frac{d\Psi}{d\xi}=\frac{\theta_T}{\overline{I}_b(\xi)}\overline{M}_b, \tag{13}$$

$$\frac{d\overline{M}_b}{d\xi}=-\theta_T\overline{Q}-r\theta_T\overline{I}_b(\xi)\overline{\omega}^2\Psi, \tag{14}$$

$$\frac{d\overline{N}}{d\xi}=r\theta_T\overline{Q}-r\theta_T A(\xi)\overline{\omega}^2\overline{U}, \tag{15}$$

$$\frac{d\overline{Q}}{d\xi}=-\frac{\theta_T}{r}\overline{N}-\theta_T\overline{A}(\xi)\overline{\omega}^2\overline{W}, \tag{16}$$

where

$$\overline{\omega}=\omega\sqrt{\frac{R^4\rho A_r}{EI_{br}}} \tag{17}$$

is the dimensionless natural frequency. This differential equation system can be shown in the matrix form as follows:

$$\frac{d\overline{\mathbf{X}}(\xi)}{d\xi}=\mathbf{B}\overline{\mathbf{X}}(\xi) \tag{18}$$

where

$$\overline{\mathbf{X}}(\xi)=\left[\overline{U}(\xi),\ \overline{W}(\xi),\ \Psi(\xi),\ \overline{N}(\xi),\ \overline{Q}(\xi),\ \overline{M}_b(\xi)\right]^T \tag{19}$$

and

$$\mathbf{B}=\begin{bmatrix} 0 & \theta_T & 0 & \theta_T/\overline{A}(\xi) & 0 & 0 \\ -\theta_T & 0 & \theta_T & 0 & \theta_T r\mu/\overline{A}(\xi) & 0 \\ 0 & 0 & 0 & 0 & 0 & \theta_T/\overline{I}_b(\xi) \\ -r\theta_T\overline{A}(\xi)\overline{\omega}^2 & 0 & 0 & 0 & r\theta_T & 0 \\ 0 & -\theta_T\overline{A}(\xi)\overline{\omega}^2 & 0 & -\theta_T/r & 0 & 0 \\ 0 & 0 & -r\theta_T\overline{I}_b(\xi)\overline{\omega}^2 & 0 & -\theta_T & 0 \end{bmatrix}. \tag{20}$$

The corresponding boundary conditions are:

- clamped left arch end
$$\overline{U}(0)=0,\ \overline{W}(0)=0,\ \Psi(0)=0, \tag{21}$$
- hinged left arch end
$$\overline{U}(0)=0,\ \overline{W}(0)=0,\ \overline{M}_b(0)=0, \tag{22}$$
- clamped right arch end
$$\overline{U}(1)=0,\ \overline{W}(1)=0,\ \Psi(1)=0, \tag{23}$$
- hinged right arch end
$$\overline{U}(1)=0,\ \overline{W}(1)=0,\ \overline{M}_b(1)=0, \tag{24}$$
- free right arch end
$$\overline{N}(1)=0,\ \overline{Q}(1)=0,\ \overline{M}_b(1)=0. \tag{25}$$

The differential equation system (18) and the relations (21)-(25) form a two-point boundary value problem of the free in-plane vibration of the circular arch with varying cross-section. The equations system (11)-(16) covers some special cases. Namely if the assumption of inextensibility of the arch centroidal line is used then the equation (11) should be replaced with:

$$\frac{d\overline{U}}{d\xi} = \theta_T \overline{W} \ . \tag{26}$$

Also, if rotatory inertia effect is ignored then the equation (14) should be replaced with:

$$\frac{d\overline{M}_b}{d\xi} = -\theta_T \overline{Q} \ . \tag{27}$$

Finally, if transverse shear effect is not considered then the equation (12) should be replaced with:

$$\frac{d\overline{W}}{d\xi} = -\overline{U}\theta_T + \theta_T \Psi \ . \tag{28}$$

3. SOLUTION PROCEDURE

In this paper the two-point boundary value problem formulated will be solved by using the symbolic-numeric method of initial parameters [24]. Since (18) represents a linear system of differential equations then its solution can be represented as:

$$\overline{\mathbf{X}}(\xi) = C_1 \overline{\mathbf{X}}_1(\xi,\overline{\omega}) + C_2 \overline{\mathbf{X}}_2(\xi,\overline{\omega}) + C_3 \overline{\mathbf{X}}_3(\xi,\overline{\omega}) \tag{29}$$

where C_1, C_2, and C_3 are the integration constants and

$$\overline{\mathbf{X}}_1(\xi,\overline{\omega}) = \Big[\overline{U}_1(\xi,\overline{\omega}),\ \overline{W}_1(\xi,\overline{\omega}),\ \Psi_1(\xi,\overline{\omega}),\ \overline{N}_1(\xi,\overline{\omega}),\ \overline{Q}_1(\xi,\overline{\omega}),\ \overline{M}_{b1}(\xi,\overline{\omega})\Big]^T , \tag{30}$$

$$\overline{\mathbf{X}}_2(\xi,\overline{\omega}) = \Big[\overline{U}_2(\xi,\overline{\omega}),\ \overline{W}_2(\xi,\overline{\omega}),\ \Psi_2(\xi,\overline{\omega}),\ \overline{N}_2(\xi,\overline{\omega}),\ \overline{Q}_2(\xi,\overline{\omega}),\ \overline{M}_{b2}(\xi,\overline{\omega})\Big]^T , \tag{31}$$

and

$$\overline{\mathbf{X}}_3(\xi,\overline{\omega}) = \Big[\overline{U}_3(\xi,\overline{\omega}),\ \overline{W}_3(\xi,\overline{\omega}),\ \Psi_3(\xi,\overline{\omega}),\ \overline{N}_3(\xi,\overline{\omega}),\ \overline{Q}_3(\xi,\overline{\omega}),\ \overline{M}_{b3}(\xi,\overline{\omega})\Big]^T \tag{32}$$

are the particular solutions obtained by integrating the differential equations system (18) using the built-in function **ParametricNDSolve[]** in Mathematica programming package with the following initial conditions, respectively:

$$\begin{array}{l} \overline{U}(0)=0,\ \overline{W}(0)=0,\ \Psi(0)=0, \\ \overline{N}(0)=1,\ \overline{Q}(0)=0,\ M_b(0)=0 \end{array} , \tag{33}$$

$$\begin{array}{l} \overline{U}(0)=0,\ \overline{W}(0)=0,\ \Psi(0)=0, \\ \overline{N}(0)=0,\ \overline{Q}(0)=1,\ M_b(0)=0 \end{array} , \tag{34}$$

and

$$\begin{array}{l} \overline{U}(0)=0,\ \overline{W}(0)=0,\ \Psi(0)=0, \\ \overline{N}(0)=0,\ \overline{Q}(0)=0,\ M_b(0)=1 \end{array} , \tag{35}$$

for the clamped left arch end, whereas for the hinged left arch end the following corresponding initial conditions are used:

$$\begin{array}{l} \overline{U}(0)=0,\ \overline{W}(0)=0,\ \Psi(0)=1, \\ \overline{N}(0)=0,\ \overline{Q}(0)=0,\ M_b(0)=0 \end{array} , \tag{36}$$

$$\begin{array}{l} \overline{U}(0)=0,\ \overline{W}(0)=0,\ \Psi(0)=0, \\ \overline{N}(0)=1,\ \overline{Q}(0)=0,\ M_b(0)=0 \end{array} , \tag{37}$$

and

$$\begin{array}{l} \overline{U}(0)=0,\ \overline{W}(0)=0,\ \Psi(0)=0, \\ \overline{N}(0)=0,\ \overline{Q}(0)=1,\ M_b(0)=0 \end{array} . \tag{38}$$

From the condition that the solution (29) satisfies the boundary conditions (23)-(25) it follows that for clamped arch right end one has:

$$\begin{array}{l} C_1\overline{U}_1(1,\overline{\omega}) + C_2\overline{U}_2(1,\overline{\omega}) + C_3\overline{U}_3(1,\overline{\omega}) = 0, \\ C_1\overline{W}_1(1,\overline{\omega}) + C_2\overline{W}_2(1,\overline{\omega}) + C_3\overline{W}_3(1,\overline{\omega}) = 0, \\ C_1\Psi_1(1,\overline{\omega}) + C_2\Psi_2(1,\overline{\omega}) + C_3\Psi_3(1,\overline{\omega}) = 0 \end{array} \tag{39}$$

whereas for hinged right arch end one has:

$$\begin{array}{l} C_1\overline{U}_1(1,\overline{\omega}) + C_2\overline{U}_2(1,\overline{\omega}) + C_3\overline{U}_3(1,\overline{\omega}) = 0, \\ C_1\overline{W}_1(1,\overline{\omega}) + C_2\overline{W}_2(1,\overline{\omega}) + C_3\overline{W}_3(1,\overline{\omega}) = 0, \\ C_1\overline{M}_{b1}(1,\overline{\omega}) + C_2\overline{M}_{b2}(1,\overline{\omega}) + C_3\overline{M}_{b3}(1,\overline{\omega}) = 0 \end{array} \tag{40}$$

and finally for the free arch right end it holds that:

$$\begin{array}{l} C_1\overline{N}_1(1,\overline{\omega}) + C_2\overline{N}_2(1,\overline{\omega}) + C_3\overline{N}_3(1,\overline{\omega}) = 0, \\ C_1\overline{Q}_1(1,\overline{\omega}) + C_2\overline{Q}_2(1,\overline{\omega}) + C_3\overline{Q}_3(1,\overline{\omega}) = 0, \\ C_1\overline{M}_{b1}(1,\overline{\omega}) + C_2\overline{M}_{b2}(1,\overline{\omega}) + C_3\overline{M}_{b3}(1,\overline{\omega}) = 0 \end{array} \tag{41}$$

The equations systems (39)-(41) represent homogeneous systems of equations in unknowns C_1, C_2, and C_3. In order that these systems can have non-trivial solutions for C_1, C_2, and C_3, the determinants of their corresponding coefficients matrix must be equal to zero, that is:

$$f_C(\overline{\omega}) \equiv \det\begin{bmatrix} \overline{U}_1(1,\overline{\omega}) & \overline{U}_2(1,\overline{\omega}) & \overline{U}_3(1,\overline{\omega}) \\ \overline{W}_1(1,\overline{\omega}) & \overline{W}_2(1,\overline{\omega}) & \overline{W}_3(1,\overline{\omega}) \\ \Psi_1(1,\overline{\omega}) & \Psi_2(1,\overline{\omega}) & \Psi_3(1,\overline{\omega}) \end{bmatrix} = 0 \ , \tag{42}$$

$$f_H(\overline{\omega}) \equiv \det\begin{bmatrix} \overline{U}_1(1,\overline{\omega}) & \overline{U}_2(1,\overline{\omega}) & \overline{U}_3(1,\overline{\omega}) \\ \overline{W}_1(1,\overline{\omega}) & \overline{W}_2(1,\overline{\omega}) & \overline{W}_3(1,\overline{\omega}) \\ \overline{M}_{b1}(1,\overline{\omega}) & \overline{M}_{b2}(1,\overline{\omega}) & \overline{M}_{b3}(1,\overline{\omega}) \end{bmatrix} = 0, \tag{43}$$

$$f_F(\overline{\omega}) \equiv \det\begin{bmatrix} \overline{N}_1(1,\overline{\omega}) & \overline{N}_2(1,\overline{\omega}) & \overline{N}_3(1,\overline{\omega}) \\ \overline{Q}_1(1,\overline{\omega}) & \overline{Q}_2(1,\overline{\omega}) & \overline{Q}_3(1,\overline{\omega}) \\ \overline{M}_{b1}(1,\overline{\omega}) & \overline{M}_{b2}(1,\overline{\omega}) & \overline{M}_{b3}(1,\overline{\omega}) \end{bmatrix} = 0 \ . \tag{44}$$

The relations (42)-(44) represent the corresponding form of frequency equations for, respectively, clamped, hinged and free right arch ends. For easier evaluation of roots of the equations (42), (43), and (44), the graphs of the functions $f_C(\overline{\omega})$, $f_H(\overline{\omega})$, and $f_F(\overline{\omega})$ obtained by using the built-in function **Plot[]** in Mathematica programming package may be used. The values of the natural frequencies can be obtained by means of the Mathematica built-in function **FindRoot[].**

4. NUMERICAL EXAMPLES

4.1. Uniform Euler-Bernoulli circular arches

In this section, the accuracy of the proposed approach in the case of the effects of axial extension, transverse shear deformation and rotatory inertia ignored is examined. For both clamped-clamped and hinged-hinged boundary conditions values of the dimensionless frequency coefficient $c=\theta_T^2\overline{\omega}$ are calculated for various values of the opening angle θ_T. These values are shown in Tables 1 and 2.

Table 1: The lowest five dimensionless frequency coefficients $c_i=\theta_T^2\overline{\omega}_i\ (i=1,...,5)$ of clamped-clamped uniform Euler-Bernoulli circular arches for $r=1/2500$ and various values of the opening angle θ_T

θ_T [rad]	Mode	[6]	This study
π/2	1	55.82523	55.82521
	2	106.7301	106.7304
	3	193.0345	193.0354
	4	284.8229	284.8374
2π/3	1	51.96935	51.96931
	2	103.5760	103.5765
	3	188.3591	188.3597
	4	281.2906	281.2913
π	1	43.27259	43.27257
	2	95.26028	95.26036
	3	176.8800	176.8810
	4	271.6560	271.6495

Table 2: The lowest five dimensionless frequency coefficients $c_i=\theta_T^2\overline{\omega}_i\ (i=1,...,5)$ of hinged-hinged uniform Euler-Bernoulli circular arches for $r=1/2500$ and various values of the opening angle θ_T

θ_T [rad]	Mode	[6]	This study
π/2	1	33.96053	33.96054
	2	79.95263	79.95272
	3	152.1706	152.1712
	4	237.9724	237.9718
2π/3	1	30.38416	30.38415
	2	76.74733	76.74741
	3	148.1494	148.1496
	4	234.5716	234.5713
π	1	22.37183	22.37184
	2	68.33021	68.33020
	3	137.9534	137.9541
	4	225.2190	225.2200

4.2. Uniform Timoshenko circular arches

In this section, the accuracy of the proposed approach in the case when the effects of axial extension, transverse shear deformation and rotatory inertia are taken into account. For both clamped-clamped and hinged-hinged boundary conditions values of the frequency coefficient $c=\theta_T^2\overline{\omega}$ are calculated for $r=1/2500$ and various values of the opening angle θ_T. These values are shown in Tables 3 and 4.

Table 3: The lowest five dimensionless frequency coefficients $c_i=\theta_T^2\overline{\omega}_i\ (i=1,...,5)$ of clamped-clamped uniform Timoshenko circular arches for $r=1/2500$ and various values of the opening angle θ_T

θ_T [rad]	Mode	[6]	This study
π/2	1	53.96596	53.96698
	2	86.19077	86.19724
	3	132.7272	132.7371
	4	175.8392	175.8474
	5	265.8141	265.8130
2π/3	1	50.93224	50.93284
	2	96.85173	96.85474
	3	178.1998	178.2048
	4	198.0489	198.0699
	5	282.9555	282.9633
π	1	42.86968	42.86991
	2	93.26808	93.26909
	3	172.2951	172.2978
	4	258.4766	258.4856
	5	372.7893	372.5899

Table 4: The lowest five dimensionless frequency coefficients $c_i=\theta_T^2\overline{\omega}_i\ (i=1,...,5)$ of hinged-hinged uniform Timoshenko circular arches for $r=1/2500$ and various values of the opening angle θ_T

θ_T [rad]	Mode	[6]	This study
π/2	1	33.46323	33.46350
	2	74.34122	74.34354
	3	121.4958	121.5088
	4	144.0231	144.0274
	5	226.3381	226.3465
2π/3	1	30.12124	30.12138
	2	74.69487	74.69574
	3	143.4124	143.4163
	4	197.2652	197.2830
	5	242.4045	242.4115
π	1	22.28359	22.28363
	2	67.67219	67.67259
	3	135.8837	135.8850
	4	219.2887	219.2796
	5	323.9065	323.8902

4.3. Timoshenko circular arches with varying cross-sections

In this section, the accuracy of our approach in the case of Timoshenko circular arches with varying cross-sections is analysed. Both unsymetric arches with varying cross-section height defined as:

$$h(\theta)=h_c(1-\eta+2\eta\theta/\theta_T),\quad 0\le\theta\le\theta_T \tag{45}$$

and symmetric arches with varying cross-section height prescribed as:

$$h(\theta)=\begin{cases}h_c(1+\eta-2\eta\theta/\theta_T), & 0\le\theta\le\theta_T/2\\ h_c(1-\eta+2\eta\theta/\theta_T), & \theta_T/2\le\theta\le\theta_T\end{cases} \tag{46}$$

are considered where h_c represents the cross-section height at the arch crown and η is the taper ratio. Note that here, the cross-section width b is constant. Also, the reference cross-section is plased at the arch crown which means that:

$$A_r=bh_c, \tag{47}$$

$$I_{br}=\frac{bh_c^3}{12}. \tag{48}$$

For both clamped-clamped and hinged-hinged boundary conditions, the corresponding values of dimensionless natural frequencies $\overline{\omega}_i\ (i=1,...,4)$ are calculated for $r=1/2500$, $\eta=0.1$, and various values of the opening angle θ_T. These values are shown in Tables 5 and 6.

Table 5: The lowest four dimensionless natural frequencies $\overline{\omega}_i(i=1,...,2)$ of tapered clamped-clamped Timoshenko symmetric circular arches for $r=1/2500$, $\eta=0.1$, and various values of the opening angle θ_T

θ_T [rad]	Mode	[9]	This study
π/18	1	433.46730	433.46807
	2	848.3639	848.3653
π/9	1	161.500908	161.502319
	2	346.5162	346.5176
π/6	1	88.1269568	88.1275550
	2	185.2505	185.2518
2π/9	1	61.7200715	61.7203672
	2	113.0604	113.0616
5π/18	1	50.8647280	50.8648687
	2	75.13195	75.13295

Table 6: The lowest four dimensionless natural frequencies $\overline{\omega}_i\ (i=1,...,4)$ of tapered hinged-hinged Timoshenko unsymmetric circular arches for $r=1/2500$, $\eta=0.1$, and various values of the opening angle θ_T

θ_T [rad]	Mode	[9]	This study
2π/9	1	48.6310055	48.6310041
	2	-	73.5871226
	3	-	159.537886
	4	-	227.199368
5π/18	1	45.66166116	45.6616819
	2	-	47.5315845
	3	-	106.612136
	4	-	172.488529
π/3	1	32.51755826	32.5176282
	2	-	44.1841916
	3	-	76.7889457
	4	-	125.924402
4π/9	1	17.59579627	17.5958086
	2	-	36.3558497
	3	-	52.0315664
	4	-	73.3148923

5. CONCLUSIONS

In this paper the symbolic-numeric method of initial parameters developed in [24] has been applied to the problem of in-plane vibration of circular arches with varying cross-sections. Through the numerical examples shown in Section 4 the effectiveness of application of the symbolic-numeric method of initial parameters to the vibration problems considered has been proved. The proposed approach allows also the vibration analysis in the case when the effects of axial extension, transverse shear deformation and rotatory inertia are ignored as well as in the case when the effects of transverse shear deformation and rotatory inertia are not included in the arch model. It is the goal of future work to expand the symbolic-numeric method of initial parameters to vibration analysis of circular arches made of functionally graded materials [10, 18-23], noncircular curved beams [3] (such as parabolic, sinusoidal, and elliptical arches) as well as arches carrying concentrated masses [26,27].

ACKNOWLEDGEMENTS

Support for this research was provided by the Ministry of Education, Science and Technological Development of the Republic of Serbia under Grant Nos. 451-03-9/2021-14/200108 and 451-03-9/2021-14/200105. This support is gratefully acknowledged.

REFERENCES

[1] P.A.A. Laura and M.J. Maurizi, "Recent Research on Vibration of Arch-Type Structures," Shock Vib. Dig, Vol. 19(1), pp. 6-9, (1987)

[2] N.M. Auciello and M.A. De Rosa, "Free Vibrations of Circular Arches: A review," J. Sound Vib, Vol. 176(4), pp. 433–458, (1994)

[3] F. Yang, R. Sedaghati and E. Esmailzadeh, "Free In-Plane Vibration of Curved Beam Structures: A Tutorial and the State of the Art," J. Vib. Control, Vol. 24(12), pp. 2400–2417, (2018)

[4] P. Chidamparam and A.W. Leissa, "Vibrations of a Planar Curved Beams, Rings and Arches," Appl. Mech. Rev, Vol. 46, pp. 467–483, (1993)

[5] M.S. Issa, T.M. Wang and B.T. Hsiao, "Extensional Vibrations of Continuous Circular Curved Beams with Rotary Inertia and Shear Deformation 1: Free vibration," J. Sound Vib, Vol. 114, pp. 297-308, (1987)

[6] E. Tufekci and A. Arpaci, "Exact Solution of In-Plane Vibrations of Circular Arches with Account Taken of Axial Extension, Transverse Shear and Rotatory Inertia Effects," J. Sound Vib, Vol. 209(5), pp. 845–856, (1998)

[7] E. Tufekci and O. Ozdemirci, "Exact Solution of Free In-Plane Vibration of a Stepped Circular Arch," J. Sound Vib, Vol. 295, pp. 725–738, (2006)

[8] F. Yang, R. Sedaghati and E. Esmailzadeh, "Free In-Plane Vibration of General Curved Beams using Finite Element Method," J. Sound Vib, Vol. 318(4-5), pp. 850-867, (2008)

[9] E. Tufekci and O.O. Yigit, "In-Plane Vibration of Circular Arches with Varying Cross-Sections," Int. J. Struct. Stab. Dyn, Vol. 13(1), pp. 1350003, (2013)

[10] S. Rajasekaran, "Static, Stability and Free Vibration Analysis of Arches Using a New Differential Transformation-Based Arch Element," Int. J. Mech. Sci, Vol. 77, pp. 82-97, (2013)

[11] U. Eroglu and E. Tufekci, "A New Finite Element Formulation for Free Vibrations of Planar Curved Beams," Mech. Based Des. Struct. Mach, Vol. 46(6), pp. 730-750, (2018)

[12] T.M. Wang and M.P. Guilbert, "Effects of rotary inertia and shear on natural frequencies of continuous circular curved beams," Int. J. Solids Struct, Vol. 17, pp. 281-289, (1981)

[13] S.Y. Lee and J.Y. Hsiao, "Free in-plane vibrations of curved non-uniform beams," Acta Mech, Vol. 155, pp. 173-189, (2002)

[14] B. Kang, C.H. Riedel and C.A. Tan, "Free vibration analysis of planar curved beams by wave propagation," J. Sound Vib, Vol. 260(1), pp. 19-44, (2003)

[15] C.H. Riedel and B. Kang, "Free vibration of elastically coupled dual-span curved beams," J. Sound Vib, Vol. 290, pp. 820-838, (2006)

[16] X. Tong, N. Mrad and B. Tabarrok, "In-Plane Vibration of Circular Arches with Variable Cross-Sections," J. Sound Vib, Vol. 212(1), pp. 121–140, (1998)

[17] G. R. Liu and T.Y. Wu, "In-Plane Vibration Analyses of Circular Arches by the Generalized Differential Quadrature Rule," Int. J. Mech. Sci, Vol. 43, pp. 2597–2611, (2001)

[18] P. Malekzadeh, "Two-Dimensional In-Plane Free Vibrations of Functionally Graded Circular Arches with Temperature-Dependent Properties," Compos. Struct, Vol. 91, pp. 38-47, (2009)

[19] S. Rajasekaran, "Free vibration of tapered arches made of axially functionally graded materials," Struct. Eng. Mech, Vol. 45(4), pp. 569–594, (2013)

[20] A.R. Noori, T.A. Aslan and B. Temel, "An Efficient Approach for In-Plane Free and Forced Vibrations of Axially Functionally Graded Parabolic Arches with Nonuniform Cross Section," Compos. Struct, Vol. 200, pp. 701-710, (2018)

[21] J.K. Lee and B.K. Lee, "In-Plane Free Vibration of Uniform Circular Arches Made of Axially Functionally Graded Materials," Int. J. Struct. Stab. Dyn, Vol. 19(8), pp. 1950084, (2019)

[22] J.K. Lee and B.K. Lee, "Free Vibration of AFG Circular Arch with Symmetric and Anti-symmetric Boundary Conditions at Mid-Arc," Symmetry, Vol. 12, pp. 417, (2020)

[23] G.S. Kim, S.J. Oh, T.E. Lee and B.K. Lee, "Free vibrations of axially functionally graded horseshoe arch," Engineering Solid Mechanics, Vol. 9, pp. 251-262, (2021)

[24] S. Šalinić, A. Obradović and A. Tomović, "Free Vibration Analysis of Axially Functionally Graded Tapered, Stepped, and Continuously Segmented Rods and Beams," Compos. B. Eng, Vol. 150, pp. 135-143, (2018)

[25] J-G. Kim, J-K. Lee and H.J. Yoon, "On the Effect of Shear Coefficients in Free Vibration Analysis of Curved Beams," J. Mech. Sci. Technol, Vol. 28(8), pp. 3181–3187, (2014)

[26] J.S. Wu, F.T. Lin and H.J. Shaw, "Free In-Plane Vibration Analysis of a Curved Beam (arch) with Arbitrary Various Concentrated Elements," Appl. Math. Model, Vol. 37, pp. 7588-7610, (2013)

[27] A. Babahammou and R. Benamarb, "Semi-Analytical Solution of In-Plane Vibrations of Circular Arches Carrying Added Point Masses," Procedia Manuf, Vol. 44, pp. 465-472, (2020)